Geometric trajectory tracking with attitude planner for vectored-thrust VTOL UAVs

Davide Invernizzi, Marco Lovera, Luca Zaccarian

Geometric trajectory tracking with attitude planner for vectored-thrust VTOL UAVs

Davide Invernizzi[1], Marco Lovera[1] and Luca Zaccarian[2]

Abstract

This paper addresses the trajectory tracking problem for VTOL UAVs in which the thrust vector can be delivered only in a fixed direction with respect to the aircraft frame. The proposed control law, based on an inner-outer loop strategy, guarantees robust tracking of a desired position trajectory. The attitude error dynamics, associated to the inner loop, is stabilized by a control torque that does not cancel non-harmful nonlinearities and that tracks at the same time a desired heading direction. This choice results in a non-autonomous feedback interconnection between the attitude and position loops, the stability of which is studied within the framework of differential inclusions. The proposed control force accounts for attitude errors to improve transient performance compared to other designs. The control scheme is tested on a multi-body model of a hexacopter UAV with actuators dynamics and aerodynamics effects, not included in the control design model.

I. INTRODUCTION

Small scale Vertical Take-Off and Landing (VTOL) UAVs have gained a large success in recent years and they are employed in numerous applications. In particular, multirotor UAVs with co-planar propellers have become popular thanks to their mechanical simplicity combined with good performance offered in many flight conditions. These vehicles belong to the class of *vectored-thrust* UAVs for which the propulsive system can deliver a control force only in a fixed direction, the thrust axis, with respect to the airframe. As a consequence, such platforms are underactuated mechanical systems in which the position dynamics can be controlled by changing the attitude of the body-fixed frame: position and attitude tasks cannot be fully decoupled. In this work, we specifically consider the problem of designing a control law that guarantees position tracking, which is mandatory in most applications involving UAVs.

The literature about trajectory tracking for UAVs is vast and the reader is referred to the survey appeared in [5] and to the references cited therein. The *vectored-thrust* dynamical model has a cascade structure in which the attitude dynamics, usually assumed fully actuated, is used as inner-loop to tilt the thrust vector in a desired direction. This direction and the thrust magnitude can be assigned by an outer-loop in charge of stabilizing the position dynamics. Furthermore, any rotational motion around the thrust force direction required for position tracking can be tracked, which is equivalent to assigning a desired heading direction. The geometric control law proposed in [7] guarantees local exponential tracking for UAVs whose propulsive system can produce both negative and positive thrust along the thrust axis. The control design presented in [4] for thrust-propelled VTOL UAVs achieves almost global tracking results. This strategy is based on a hierarchical design that considers the angular velocity as an intermediate control input, by relying on a sufficiently large time-scale separation between the attitude and position loops. Inner-outer loop paradigms, which combine a nested saturations stabilizer for the position dynamics and a hybrid approach to stabilize the attitude error dynamics, are employed in [10]. The control law presented therein, which ensures robust global tracking, relies on an exosystem to study the stability of the attitude subsystem.

Our work takes inspiration from [11], in which the emphasis was on defining classes of position and attitude controllers that stabilize the system at a given position (constant reference). In particular, we tackle attitude tracking by selecting a control torque that does not cancel non-harmful nonlinearities and that has a simpler expression than the ones usually employed for UAV attitude control [7]. This choice is a representative candidate for a large class of admissible attitude control laws that guarantee uniform asymptotic tracking (UAT). Then, by designing a control force that guarantees a (small signal) Input-to-State Stability (ISS) property for the perturbed position error dynamics, the stability of the resulting feedback interconnection is studied within the framework of differential inclusions. This approach simplifies the analysis of the corresponding non-autonomous system: the proof technique relies on casting the control problem as a stability problem for a compact attractor with dynamics satisfying regularity conditions that ensure robustness of the stability property against a very large class of (sufficiently small) perturbations [3, Chapter 7]. The control law guarantees robust tracking under mild smoothness and boundedness properties of the desired trajectory with no restriction on the initial position error and with some relatively standard restrictions on the initial attitude error. Furthermore, the computation of the reference attitude required to stabilize the position dynamics accommodates the heading direction tracking task and avoids, by design, possible degenerate conditions that are present in the solution proposed in [7]. Finally, we introduce an attitude error dependent term in the definition of the control force, which is shown to reduce significantly the position overshoot when the initial attitude error is large.

[1]Davide Invernizzi and Marco Lovera are with Dipartimento di Scienze e Tecnologie Aerospaziali, Politecnico di Milano, Via La Masa 34, 20156 Milano, Italy {davide.invernizzi, marco.lovera}@polimi.it

[2]Luca Zaccarian is with CNRS, LAAS, 7 avenue du colonel Roche, F-31400 Toulouse, France, Univ. de Toulouse, LAAS, F-31400 Toulouse, France, and Dipartimento di Ingegneria Industriale, University of Trento, Italy. zaccarian@laas.fr

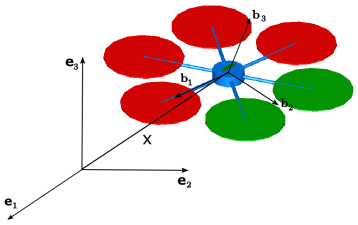

Fig. 1. Reference frame definition.

Notation. For $A \in \mathbb{R}^{n\times n}$, the minimum and maximum eigenvalues are denoted as $\lambda_m(A)$ and $\lambda_M(A)$, respectively, and $\text{skew}(A) := \frac{A-A^T}{2}$ is the skew-symmetric part of A. The unit vectors corresponding to the canonical basis in $\mathbb{R}^n$ are $e_i := [0,\dots,1,\dots,0]^T$ for $i = 1, ..., n$. The identity matrix in $\mathbb{R}^{n\times n}$ is denoted as $I_n := [e_1, \cdots e_i \cdots, e_n]$. The notation $R_u(\theta)$ is used to represent the rotation matrix corresponding to a rotation about a unit axis $u \in \mathbb{S}^2$ of an angle $\theta \in \mathbb{R}$. Given the vectors x, y we often denote $(x,y) := [x^T, y^T]^T$. Given $\omega \in \mathbb{R}^3$, the *hat* map $\hat{\cdot} : \mathbb{R}^3 \to \mathfrak{so}(3) := \{\Omega \in \mathbb{R}^{3\times3} : \Omega = -\Omega^T\}$ is such that $\hat{\omega} y = \omega \times y$, $\forall y \in \mathbb{R}^3$. The inverse of the *hat* map is the *vee* map, denoted as $(\cdot)^\vee : \mathfrak{so}(3) \to \mathbb{R}^3$. K is the class of function $\mathbb{R}_{\geq0} \to \mathbb{R}_{\geq0}$ which are zero at zero, strictly increasing, and continuous. K_∞ is the subset of class-K functions that are unbounded. KL is the class of functions $\mathbb{R}_{\geq0} \times \mathbb{R}_{\geq0} \to \mathbb{R}_{\geq0}$ which are class-K in the first argument and decreasing and converging to zero as their second argument tends to $+\infty$.

II. MATHEMATICAL MODELING

The configuration of a UAV is globally and uniquely described by the pair $(R,x) \in \text{SO}(3) \times \mathbb{R}^3$, where R and x are, respectively, the rotation matrix and the position vector of a body-fixed frame $\mathscr{F}_B = (O_B, \{b_1, b_2, b_3\})$ with respect to an inertial frame $\mathscr{F}_I = (0_I, \{e_1, e_2, e_3\})$ (Figure 1). The well-known equations of motion for control design are [9]:

$$\dot{x} = v \tag{1}$$
$$\dot{R} = R\hat{\omega} \tag{2}$$
$$m\dot{v} = -mge_3 + Rf_c \tag{3}$$
$$J\dot{\omega} = -\hat{\omega}J\omega + \tau_c, \tag{4}$$

where $\omega \in \mathbb{R}^3$ is the *body* angular velocity, $v \in \mathbb{R}^3$ is the translational velocity of the center of mass, resolved in $\mathscr{F}_I$, $m \in \mathbb{R}_{>0}$ and $J = J^T \in \mathbb{R}^{3\times3}_{>0}$ are the mass and the inertia matrix of the rigid body, respectively and $(f_c, \tau_c) \in \mathbb{R}^6$ are the control force and torque resolved in $\mathscr{F}_B$. These equations may be employed to design control laws for a large class of small-scale UAVs in which the components are sufficiently rigid, the flight conditions are such that aerodynamic effects can be dominated with high gain control and the actuators dynamics is fast enough. The propulsive system of vectored-thrust VTOL UAVs allows to produce a control force directed only along the positive direction of $b_3 := Re_3$, *i.e.*, its components in the body frame must satisfy:

$$f_c = T(t)e_3, \quad 0 < T(t) \leq T_M, \quad \forall t \geq 0 \tag{5}$$

where $T \in \mathbb{R}_{>0}$ is the thrust magnitude. It is usually assumed that the control torque τ_c spans $\mathbb{R}^3$, *i.e.*, the rotational dynamics (2), (4) is *fully actuated*.

III. CONTROL PROBLEM

This work deals with the tracking control problem for the system described by (1)-(4). It is well known that it is not possible for vectored-thrust UAVs to track an arbitrary full pose trajectory $t \mapsto (R_d(t), x_d(t)) \in \text{SO}(3) \times \mathbb{R}^3$. To show this formally, let us compute the nominal control wrench, which is obtained by inverting the system dynamics evaluated at the reference, *i.e.*:

$$f_c^{ss}(t) := mR_d^T(t)\left(\dot{v}_d(t) + ge_3\right) \tag{6}$$
$$\tau_c^{ss}(t) := J\dot{\omega}_d(t) + \hat{\omega}_d(t)J\omega_d(t). \tag{7}$$

Notice that f_c^{ss} will be compatible with the constraint in equation (5) if and only if $b_{d_3} := R_d e_3$ is aligned with the vector $m(\dot{v}_d + ge_3)$, namely $b_{d_3}(t) = \frac{\dot{v}_d(t)+ge_3}{\|\dot{v}_d(t)+ge_3\|}$. In this case, the position tracking objective can be achieved whereas the attitude one can be partially realized: only an arbitrary rotation around b_{d_3} is compatible with the constraint. Indeed, given a feasible R_d, $R_d R_{e_3}(\psi_d)$ is feasible as well: $f_c^{ss} = R_{e_3}^T(\psi_d)R_d^T m(\dot{v}_d + ge_3) = \{0, 0, \|m(\dot{v}_d + ge_3)\|\}$. In this case, the steady state force is in the form $f_c^{ss} = Te_3$, with $T = \|m(\dot{v}_d + ge_3)\|$. If one is willing to relax the position tracking objective, attitude tracking of an arbitrary set-point is feasible but only the desired vertical motion x_{d_3} can be freely assigned. While the latter flight

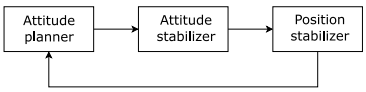

Fig. 2. Feedback interconnection (error dynamics).

condition may be used, safely, only for short maneuvers, most applications involving UAVs require position tracking. In the following, we will refer to the reduced tracking problem on $\mathbb{R}^3 \times \mathbb{S}^1$, which will be embedded on $\mathrm{SO}(3) \times \mathbb{R}^3$ via a proper mapping $\mathbb{S}^1 \to \mathrm{SO}(3)$. Specifically, we will introduce a reference attitude $R_p \in \mathrm{SO}(3)$, which is the output of an attitude planner, that is computed in order to be compliant with the constraint (5) and to guarantee the fulfillment of the reduced attitude tracking problem.

The following assumptions are required to hold for the desired trajectory.

Assumption 1: Smoothness, boundedness and trackability of the desired trajectory. Given a trajectory $t \mapsto (R_d(t), x_d(t), v_d(t), \omega_d(t)) \in \mathrm{SO}(3) \times \mathbb{R}^9$, where $v_d(t) := \dot{x}_d(t)$ and $\omega_d(t) := (R_d(t)^T \dot{R}_d(t))^\vee$, the following conditions hold:

1) the position trajectory $x_d(\cdot)$ belongs at least to C^4;
2) the acceleration $\dot{v}_d(\cdot)$ and jerk $\ddot{v}_d(\cdot)$ belong to L_∞; in particular, $\dot{v}_d(\cdot)$ is such that f_c^{ss} defined in (6) is bounded by $0 < f_m^{ss} \leq \|f_c^{ss}(t)\| \leq f_M^{ss} < T_M \ \forall t \geq 0$, where T_M is defined in (5), and $\inf_{t \geq 0}(m|g + \dot{v}_{d_3}(t)|) > 0$.
3) the attitude $R_d(\cdot)$ satisfies $R_d(t)e_3 = \frac{\dot{v}_d(t)+ge_3}{\|\dot{v}_d(t)+ge_3\|} \ \forall t \geq 0$;
4) the angular velocity is bounded and continuously differentiable, *i.e.*, $\omega_d(\cdot) \in C^1 \cap L_\infty$.

IV. ROBUST TRACKING DESIGN

In this section we present the design of a control law that ensures robust tracking of any desired trajectory satisfying Assumption 1 with no restriction on the initial position error and some reasonable restriction on the initial attitude error. The resulting closed-loop is a feedback interconnection in which an attitude planner provides the reference to the attitude subsystem which, in turn, affects the position error dynamics (Figure 2).

A. Control force and position error dynamics

According to the dynamics in (1)-(4), the natural choice of the tracking errors for position and velocity is expressed in the inertial frame:

$$e_x := x - x_d \quad e_v := v - v_d. \tag{8}$$

The control objective is to stabilize $(e_x, e_v) = (0,0)$. Consider equations (1), (3) and the definition of the errors in (8). Then,

$$\dot{e}_x = e_v \tag{9}$$

$$m\dot{e}_v = m(\dot{v} - \dot{v}_d) = -m(\dot{v}_d + ge_3) + Rf_c. \tag{10}$$

The system would be fully actuated if one could arbitrarily assign f_c, and if it would be possible to enforce $Rf_c = f_d$, with

$$f_d := \beta(e_x, e_v) + m(\dot{v}_d + ge_3), \tag{11}$$

where $\beta : \mathbb{R}^6 \to \mathbb{R}^3$ is a static state feedback stabilizer. The corresponding closed-loop dynamics would be described by (9) and $m\dot{e}_v = \beta(e_x, e_v)$. Thus, the zero equilibrium would be globally asymptotically stable for a suitable choice of β. As it is not possible to obtain $Rf_c = f_d$ under constraint (5), it is convenient to rewrite the velocity error dynamics as:

$$m\dot{e}_v = -m(\dot{v}_d + ge_3) + RR_p^T R_p f_c \tag{12}$$

$$= -m(\dot{v}_d + ge_3) + R_e R_p f_c \tag{13}$$

where

$$R_e := RR_p^T \in \mathrm{SO}(3) \tag{14}$$

is the so-called left attitude error [1]. Introducing the corresponding angular velocity error,

$$e_\omega := \omega - \omega_p, \tag{15}$$

a natural choice for the control force f_c is

$$f_c := R_p^T \Phi(R_e, e_\omega, t) f_d \tag{16}$$

where $\Phi(R_e, e_\omega, t) : T\mathrm{SO}(3) \times \mathbb{R}_{\geq 0} \to \mathbb{R}^{3\times 3}$, $T\mathrm{SO}(3) := \mathrm{SO}(3) \times \mathbb{R}^3$ is the tangent bundle of $\mathrm{SO}(3)$. Indeed, by adding and subtracting f_d in equation (13), one gets:

$$m\dot{e}_v = \beta(e_x, e_v) + \Delta R(R_e, e_\omega, t) f_d(e_x, e_v, \dot{v}_d) \tag{17}$$

where

$$\Delta R(R_e, e_\omega, t) := R_e \Phi(R_e, e_\omega, t) - I_3. \tag{18}$$

The position error is affected by the attitude error through the term $\Delta R f_d$, which weighs the mismatch between the desired force f_d and the control force resolved in $\mathscr{F}_I$, *i.e.*, $R f_c$.

Remark 1: The explicit dependence on time in the definition of $\Phi(R_e, e_\omega, t)$ in equation (16) gives more freedom in the tuning of the control action in the transient phase. In particular, when then attitude error is large, the term Φ can be exploited to reduce the control force and correspondingly limit the overshoot in the position tracking.

The rationale behind the proposed control law is that if the desired attitude error equilibrium can be made asymptotically stable, then, for $t \to \infty$, $R_e(t) \to I_3$, $\Phi(R_e(t), e_\omega(t), t) \to I_3$ and the term $R(t) f_c(t) = R_e(t)\Phi(t) f_d(t) \to f_d(t)$, which is the force, in the inertial frame, required to track the desired position trajectory. Indeed, in this case, the mismatch between the desired and actual control force converges to zero as well, namely $\Delta R(t) f_d(t) \to 0$. However, to prove this idea, we have to study the stability of the complete system, including the attitude error dynamics. In particular, we have to make assumptions on the attitude error dependent matrix Φ and on the feedback stabilizer β in equations (18)-(17), so that the position error dynamics have certain desired properties. First of all, the choice of Φ must be such that the following property holds true for the attitude mismatch ΔR.

Property 1: (Vanishing perturbations). Consider ΔR defined in equation (18). Given $V_a(R_e, e_\omega) := \sqrt{\|e_\omega\|^2 + \Psi^2(R_e)}$, where $\Psi(R_e) := \sqrt{\frac{1}{4}\mathrm{tr}(I_3 - R_3)}$, there exists a bounded class-K function $\gamma : \mathbb{R}_{\geq 0} \to \mathbb{R}_{\geq 0}$, satisfying $\forall (R_e, e_\omega, t) \in T\mathrm{SO}(3) \times \mathbb{R}_{\geq 0}$:

$$\|\Delta R(R_e, e_\omega, t)\| \leq \gamma(V_a(R_e, e_\omega)). \tag{19}$$

A convenient choice of Φ is to employ a scaling transformation, dependent on the attitude error alone, as follows:

$$\Phi(R_e, e_\omega, t) := c(R_e, e_\omega, t) I_3, \tag{20}$$

where $c : T\mathrm{SO}(3) \times \mathbb{R}_{\geq 0} \to \mathbb{R}_{\geq 0}$ is a suitably selected scaling function. Property 1 is needed to ensure that, at convergence, the magnitude of the delivered control force f_c in (16) converges to the nominal force f_c^{ss} (6). The next proposition gives an example of function c, which is naturally written in terms of the angle θ_e between the planner axis $b_{p_3} := R_p e_3$ and the body axis b_3:

$$\theta_e(R_e, R_p) := \arccos(b_{p_3}^T b_3) = \arccos(e_3^T R_p^T R_e R_p e_3). \tag{21}$$

Proposition 1: Given $c(R_e, t) := \frac{\ell - (1 - \cos(\theta_e(R_e, R_p(t))))}{\ell}$, where θ_e is defined in (21), then, for $\Phi(R_e, e_\omega, t) := c(R_e, t) I_3$ and $\ell > 2$, Property 1 is satisfied.

Proof: The proof is similar to the one of [6, Prop. 4]. ∎

We now state the main properties concerning the choice of the feedback stabilizer.

Property 2: Consider the closed-loop position dynamics (9), (17) and Assumption 1. The feedback stabilizer β in equation (11) is such that:

1) $\beta(\cdot,\cdot) \in L_\infty \cap C^2$ and, given $\beta_{i_M} \in \mathbb{R}_{>0} : |\beta_i(e_x, e_v)| \leq \beta_{i_M}$, $\forall (e_x, e_v, i) \in \mathbb{R}^6 \times \{1,2,3\}$, it holds that:

$$\max_{i=1,2,3} \beta_{i_M} < \min\left(\frac{T_M - f_M^{ss}}{\sqrt{3}}, \inf_{t \geq 0}(m|g + \dot{v}_{d_3}(t)|) \right), \tag{22}$$

   where T_M is defined in (5) and f_M^{ss} in Assumption 1-3.
2) $\nabla\beta(\cdot,\cdot) \in L_\infty$, and $\nabla\beta_{e_x}(e_x, e_v) = 0_{3\times 3}\ \forall (e_x, e_v) \in \Omega_p := \left\{ (e_x, e_v) \in \mathbb{R}^6 : \|e_v\| \geq e_M \right\}$, for some $e_M \in \mathbb{R}_{>0}$.
3) the position error dynamics is small signal ISS, *i.e.*, there exists $\varepsilon \in \mathbb{R}_{>0}$ such that, given any piecewise continuous perturbation $t \mapsto \Delta(t) \in \mathbb{R}^3 : \|\Delta(t)\| < \varepsilon\ \forall t \geq t_0 \geq 0$, the solution of (9) and $m\dot{e}_v = \beta(e_x, e_v) + \Delta(t)$ satisfies $\|(e_x(t), e_v(t))\| \leq \alpha(\|(e_x(0), e_v(0))\|, t - t_0) + \mu(\|\Delta\|_\infty)$ for some $\alpha(\cdot,\cdot) \in KL$, $\mu(\cdot) \in K$ and $\forall (e_x(0), e_v(0)) \in \mathbb{R}^6$, $\forall t \geq t_0$.

In this work we will employ the nested saturation stabilizer of [10], which satisfies all the above properties:

$$\beta(e_x, e_v) := \lambda_2 \mathrm{sat}\left(\frac{k_2}{\lambda_2} \left(e_v + \lambda_1 \mathrm{sat}\left(\frac{k_1}{\lambda_1} e_x \right) \right) \right), \tag{23}$$

where k_1, k_2 are stabilizing gains and λ_1, λ_2 are suitably chosen saturation levels [10, Prop. 1].

B. Control torque and attitude error dynamics

The attitude controller has to ensure the convergence of the attitude tracking errors according to the fully actuated rotational dynamics in equations (2), (4). We consider a reference trajectory $(R_p, \omega_p) \in T\mathrm{SO}(3)$ for which $\omega_p(\cdot) = (R_p^T(\cdot)\dot{R}_p(\cdot))^\vee \in C^1 \cap L_\infty$. Consider the control law

$$\tau_c = -R_p^T e_R - K_\omega e_\omega + J\dot{\omega}_p + \hat{\omega}_p J\omega, \tag{24}$$

where $K_\omega \in \mathbb{R}^{3\times3}$ is positive definite and $e_R := \text{skew}(K_R R_e)^\vee$ is the left-trivialized derivative of the navigation function $\Psi_{K_R}(R_e) := \frac{1}{2}\text{tr}(K_R(I-R_e))$. Combining the control torque (24) with the rotational equations of motion (2)-(4), the dynamics of the errors (14) and (15) evolves as:

$$\dot{R}_e = R_e R_p \hat{e}_\omega R_p^T \tag{25}$$

$$J\dot{e}_\omega = -R_p^T e_R - K_\omega e_\omega - \hat{e}_\omega J e_\omega - \hat{e}_\omega J \omega_p. \tag{26}$$

The control torque (24), first proposed by [1], has a simpler expression than the one based on the right group error considered in [7] and no cancellation of non-harmful nonlinearities occurs. The equilibrium points for the attitude subsystem are the points where the differential e_R of Ψ_{K_R} and the angular velocity error vanish, namely $(e_R, e_\omega) = (0,0)$. This set of equilibria contains the desired equilibrium $(R_e, e_\omega) = (I_3, 0)$ and additional undesired configurations corresponding to the other critical points of Ψ_{K_R}. This is intrinsic to the structure of SO(3): as is well known, no continuous time-invariant control law can globally stabilize the identity element. Nonetheless, by defining the positive constant $\ell_R := \lambda_m(\text{tr}(K_R)I_3 - K_R)$ it is possible to show that in the sublevel set $S_R := \{R_e \in \text{SO}(3) : \Psi_{K_R}(R_e) < \ell_R\}$ the point $R_e = I_3$ is the unique critical point and minimum of Ψ_{K_R}. We can state the following result which extends [1, Lem. 9] and the proof is omitted due to space limitations.

Theorem 1: Consider the system described by (25)-(26) controlled by (24) and a reference attitude $t \mapsto (R_p(t), \omega_p(t)) \in T\text{SO}(3)$, such that $\omega_p(\cdot) := (R_p^T(\cdot)\dot{R}_p(\cdot))^\vee \in C^1 \cap L_\infty$. For any symmetric matrix $K_R \in \mathbb{R}^{3\times3}$ such that $(\text{tr}(K_R)I_3 - K_R) \in \mathbb{R}^{3\times3}_{>0}$ and any matrix $K_\omega \in \mathbb{R}^{3\times3}_{>0}$, the equilibrium point $(R_e, e_\omega) = (I_3, 0)$ is robustly uniformly asymptotically stable with basin of attraction containing the set $S_a := \{(R_e, e_\omega) \in T\text{SO}(3) : V_R(R_e, e_\omega) < \ell_R\}$ where $\ell_R := \lambda_m(\text{tr}(K_R)I_3 - K_R)$ and $V_R(R_e, e_\omega) := \frac{1}{2}e_\omega^T J e_\omega + \Psi_{K_R}(R_e)$.

C. Attitude planner

The attitude planner is in charge of producing the reference attitude $(R_p, \omega_p) \in T\text{SO}(3)$ so that the control force is compatible with the actuation constraint and the desired heading direction is tracked.

The control force computed in (16) has to satisfy the actuation constraint (5), namely, for some $T \in \mathbb{R}_{>0}$,

$$f_c = c(R_e, e_\omega, t) R_p^T f_d = T e_3. \tag{27}$$

By selecting the third planner axis as $b_{p_3} := \frac{f_d}{\|f_d\|}$ the constraint (5) is readily verified with $T = c(R_e, e_\omega, t)\|f_d\|$. Indeed, in vector form, one gets:

$$c(R_e, t) \begin{bmatrix} b_{p_1}^T f_d \\ b_{p_2}^T f_d \\ b_{p_3}^T f_d \end{bmatrix} = \begin{bmatrix} 0 \\ 0 \\ c(R_e, e_\omega, t)\|f_d\| \end{bmatrix}, \tag{28}$$

because b_{p_1}, b_{p_2} must be chosen orthogonal to b_{p_3} to have a well defined rotation matrix R_p. Selecting b_{p_3} as above fixes two out of three parameters in the definition of R_p and the remaining one can be exploited to fulfill the heading direction tracking task. A viable choice is

$$R_p = R_c R_{e_3}(\psi_d), \quad R_c := \begin{bmatrix} b_{p_2} \times b_{p_3} & \frac{b_{p_3} \times e_1}{\|b_{p_3} \times e_1\|} & b_{p_3} \end{bmatrix}, \tag{29}$$

or alternatively the one proposed in [7]:

$$R_p := \begin{bmatrix} b_{p_2} \times b_{p_3} & \frac{b_{p_3} \times b_d}{b_{p_3} \times b_d} & b_{p_3} \end{bmatrix}, \tag{30}$$

where $b_d(t) := \begin{bmatrix} \cos(\psi_d(t)) & \sin(\psi_d(t)) & 0 \end{bmatrix}^T$, where $t \mapsto \psi_d(t) \in \mathbb{S}^1$ is the desired yaw angle (used to generate $R_d(t)$).

The definitions of R_p in equation (29) or (30) become both indeterminate in the degenerate cases when $\|f_d\| = 0$ and b_{p_3} is parallel to e_1 or b_d. These issues have not been addressed in the pioneering work of [7] but only recently (for the first degenerate case) in [10]. We propose a solution that solves the issues altogether. First of all, by referring to Property 2-1 of β, we can write the following inequality $\|f_d(t)\| \geq |f_{d_3}(t)| \geq \inf_{t\geq0}(m|g + \dot{v}_{d_3}(t)|) - \beta_{3_M} > 0 \ \forall t \geq 0$. To ensure that the term $\|b_{p_3} \times b_d\|$ does not vanish, it is enough to choose the reference heading direction b_d in the horizontal plane (e_1, e_2), as done in equation (29) or (30). Indeed, the cross product will never result in the zero vector because the third component of b_{p_3} is always different from zero.

Lemma 1: (Feasibility conditions of the reference attitude). If the desired reference satisfies Assumption 1 and $\beta(\cdot,\cdot)$ is selected according to Property 2, then, the planner output $t \mapsto (R_p(t), \omega_p(t))$, where $R_p(t)$ is obtained according to equations (29) or (30) and $\omega_p(t) := (R_p(t)^T \dot{R}_p(t))^\vee$, is feasible, in the sense that $\omega_p(\cdot) \in C^1 \cap L_\infty \ \forall t \geq 0$.

Proof: The proof is similar to the one presented in [10] and it exploits Property 2-1 and 2-2. Note that we do not require boundedness of the planner angular velocity. ■

V. Stability analysis of the complete dynamics

This section presents the main results of the stability analysis for the complete system. Our proof is based on a compact representation of the closed loop wherein the solutions of the time-varying dynamics is embedded into a time-invariant differential inclusion, in ways that are similar to the strategy in [10], even though the approach adopted here does not require the (somewhat stringent) assumption that $\dot{\omega}_p$ must be bounded. By introducing $x_a := (R_e, e_\omega) \in T\mathrm{SO}(3)$ and $x_p := (e_x, e_v) \in \mathbb{R}^6$, the solutions to the attitude error dynamics (25)-(26) and the position error dynamics (9), (17) can be embedded within the solution generated by the following constrained differential inclusion:

$$(A) \quad \dot{x}_a \in F_a(x_a), \qquad x_a \in T\mathrm{SO}(3) \tag{31}$$

$$(P) \quad \dot{x}_p \in F_p(x_p, x_a), \qquad x_p \in \mathbb{R}^6, \tag{32}$$

where we used a slight abuse of notation[1] and $F_a(x_a)$, $F_p(x_p)$ are defined as

$$F_a(x_a) := \bigcup_{\substack{R_p \in \overline{\mathrm{co}}(\mathrm{SO}(3)) \\ \|\omega_p\| \le \omega_M}} \begin{bmatrix} R_e R_p \hat{e}_\omega R_p^T \\ -J^{-1}\left(R_p^T e_R + K_\omega e_\omega + \hat{e}_\omega J e_\omega + \hat{e}_\omega J \omega_p\right) \end{bmatrix}, \tag{33}$$

$$F_p(x_p, x_a) := \begin{bmatrix} e_v \\ \frac{1}{m}\left(\beta(e_x, e_v) + f_M \gamma(V_a(R_e, e_\omega))\overline{\mathscr{B}_3}\right) \end{bmatrix} \tag{34}$$

where $\overline{\mathrm{co}}(\cdot)$ denotes the closed convex hull, $\overline{\mathscr{B}_3}$ denotes the closed unit ball and $\omega_M \in \mathbb{R}_{>0}$ is a constant whose existence is ensured by Assumption 1. Moreover, function γ comes from (19), and scalar $f_M := \sqrt{3}\max_{i=1,2,3}\beta_{i_M} + f_M^{ss}$ is a bound on the term f_d defined in equation (11) which holds thanks to Assumption 1 and Property 2.

Based on representation (31), (32), asymptotic tracking for the complete dynamics can be proven, under Assumption 1, as stated by the following Theorem.

Theorem 2: Consider the closed-loop system described by (9), (17), (25), (26) controlled by (16), (24), a desired trajectory $t \mapsto (R_d(t), \omega_d(t), x_d(t), v_d(t))$ satisfying Assumption 1 and the planner output (R_p, ω_p) given by equation (29) or (30) and $\omega_p = (R_p^T \dot{R}_p)^\vee$. Assume that $c(\cdot,\cdot,\cdot)$ is such that $\Phi(\cdot,\cdot,\cdot)$ given in (20) satisfies Property 1 and $\beta(\cdot,\cdot)$ in (11) is selected according to Property 2. Then, the control force (16) satisfies equation (5) and, for any symmetric matrix K_R such that $(\mathrm{tr}(K_R)I_3 - K_R) \in \mathbb{R}^{3\times3}_{>0}$, any $K_\omega \in \mathbb{R}^{3\times3}_{>0}$, the point $(R_e, e_\omega, e_x, e_v) = (I_3, 0, 0, 0)$ is robustly uniformly asymptotically stable with domain of attraction containing $S_a \times \mathbb{R}^6$, where S_A is defined in Theorem 1.

Proof: The feedback interconnection (31), (32) comprises the (static) attitude planner, the attitude subsystem (31), the stability properties (with domain of attraction S_a) of which have been established in Theorem 1, and the position subsystem (32), which is stabilized by function β, which satisfies Property 2. First, note that the planner output matches the condition of Theorem 1 thanks to Lemma 1. Then, (local) stability of the cascade between the attitude and position subsystems follows from reduction theorems for differential inclusions (see, *e.g.*, [8]) whereas attractivity from $S_a \times \mathbb{R}^6$ can be established using the small signal ISS properties of stabilizer (23) following the same steps as in [10, Proof of Prop. 4]. Finally, stability and attractivity of the point $(R_e, e_\omega, e_x, e_v) = (I_3, 0, 0, 0)$ for the closed-loop implies *KL* asymptotic stability from [3, Thm 7.12], and then also robust *KL* asymptotic stability from [3, Thm 7.21]. Finally, the control force f_c defined in (16) with R_p given by (29) or (30), automatically satisfies constraint (5) as shown in (28). ■

VI. Numerical results

In this section two simulation examples are presented. We refer to a hexarotor UAV (Figure 1), which is an aerial vehicle equipped with six propellers. This system has six control inputs (the rotor angular velocities $\{\Omega_{r_1}, \cdots, \Omega_{r_6}\}$ that can be exploited to apply the required control (f_c, τ_c) according to equations (24), (16). In particular, the mixer map that relates the actual inputs and the control action is pseudo-invertible as shown in [2]. The simulation model is a multi-body system with seven rigid-bodies, developed in the Modelica modelling language, augmented to include the dynamics of the motor/propeller groups (first-order models). Furthermore, body-drag and induced-drag forces are accounted for as well as the aerodynamic damping torque by the disturbance wrench $(f_e, \tau_e) \in \mathbb{R}^6$. Specifically, we consider simplified models $\tau_e := D_a\omega$ where $D_a = -\mathrm{diag}(0.04, 0.04, 0.02)$, and $f_e := -c_d\|v\|v - \sum_{i=1}^6 c_I\sqrt{T_i}(v_i - (v_i^T b_3)b_3)$ where $c_d = 0.01$, $c_I = 0.05$ are the body and induced drag coefficients, respectively, v_i is the velocity of the hub of the *i-th* rotor and T_i is the thrust delivered by the *i-th* rotor. For the sake of conciseness, only the nominal values used for the control tuning are reported: $J = \mathrm{diag}\,(0.008, 0.008, 0.016)\,\mathrm{kg\,m^2}, m = 1\mathrm{kg}$. The controller gains are $K_R = 0.9I_3$, $K_\omega = 0.1I_3$, $\ell = 2.1$, $\lambda_2 = 9$, $\lambda_1 = 1$, $k_1 = 0.06$ and $k_2 = 9$.

[1] To be consistent with the formulation, the differential inclusion should be written by exploiting the vectorization, $\mathrm{vec}(\dot{R}_e) \in \mathrm{vec}\,(F_R(R_e, e_\omega))$

A. Eight-shaped trajectory tracking

We consider the eight-shaped trajectory, $x_d(t) = \left[\begin{array}{ccc} \frac{\sin(2\omega_s t)}{3-\cos(2\omega_s t)} & \frac{2\cos(\omega_s t)}{3-\cos(2\omega_s t)} & 1 \end{array}\right]^T$ m with $\omega_s = \frac{2\pi}{12}\,\mathrm{rad\,s^{-1}}$, whilst the desired heading direction is $b_d(t) = e_1$. The reference trajectory (dotted line) is shown in the small box in Figure 3, together with the actual path of the rigid body (solid line) for five rounds, starting from a misplaced hovering condition at $x(0) = [1.2\ 0\ 1]^T$ m. The attitude tracking performance is illustrated in Figure 4. It is clear that even in the presence of unmodeled dynamics, the tracking errors are bounded.

B. Trajectory tracking with large attitude error recovery

Let us consider the case of an attitude recovery maneuver to show the benefit that can be gained by exploiting the scaling factor $c(R_e, e_\omega, t)$ introduced in the control force (16). The initial conditions correspond to the hexacopter being dropped with the reference plane perpendicular to the ground: $x(0) = [0\ 0\ 1]^T$ m, $v(0) = [0\ 0\ 0]^T\,\mathrm{m\,s^{-1}}$ and $R(0) = R_{e_2}\left(\frac{\pi}{2}\right)$, $\omega(0) = [0\ 0\ 0]^T\,\mathrm{rad\,s^{-1}}$. The set-point is the hovering condition at $x(0) = [0\ 0\ 1\ ]^T$ m. We compare the results obtained by selecting $c(R_e, e_\omega, t)$ as in Proposition 1 with the standard choice $c(R_e, e_\omega, t) = 1$ [10]. Note that the approach in [7] cannot be tested since it would result in $\|f_c\| = 0\,\mathrm{N}$. The corresponding term has a scaling effect on the magnitude of the delivered control force, which cannot be instantaneously directed as the desired control force f_d in (11) due to the underactuation. While the thrust axis b_3 is converging to the direction of f_d thanks to the attitude stabilizer (24), the position overshoot is dependent on the magnitude of the control force and the scaling effect introduced by function c limits this unwanted effect. Figure 5 shows that the percentage difference of overshoot in the position tracking is reduced of about 50% with respect to the case without scaling.

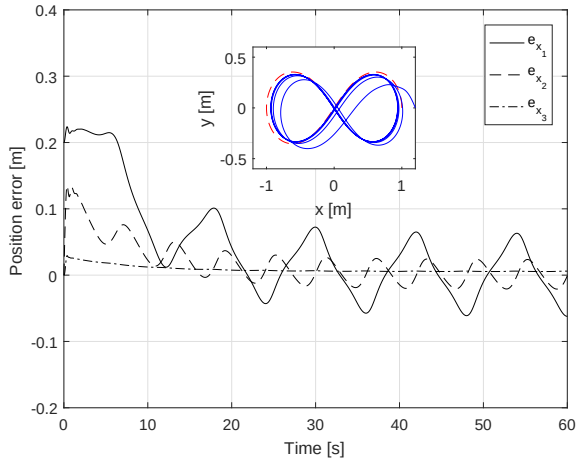

Fig. 3. (A) Position tracking error - e_x.

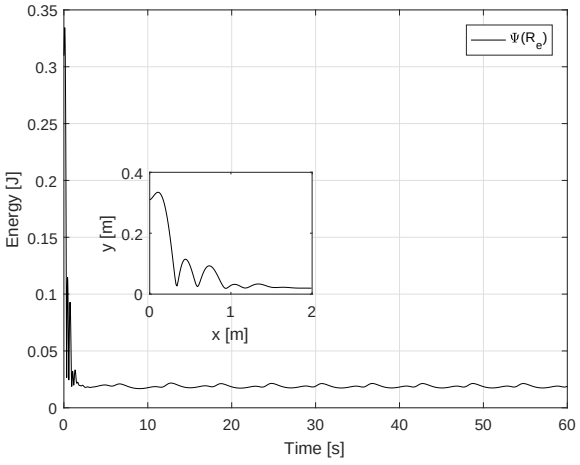

Fig. 4. (A) Attitude tracking error - $\Psi(R_e) := \sqrt{\frac{1}{4}(I_3 - R_e)}$.

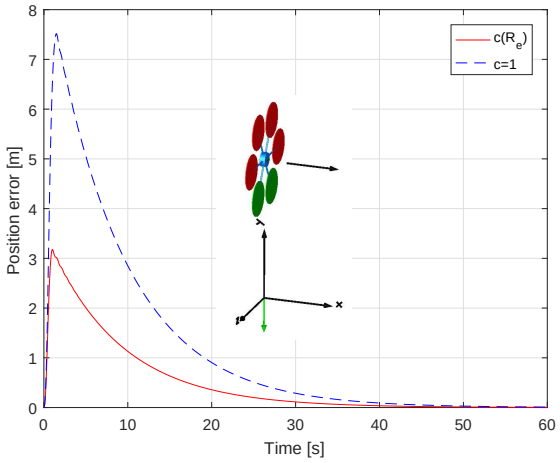

Fig. 5. (B) Position errors comparison - $\|e_x\|$.

VII. CONCLUSIONS

In this paper the trajectory tracking control problem for underactuated VTOL UAVs has been addressed. The proposed approach relies on an inner-outer loop paradigm in which the attitude subsystem stabilizes the position error dynamics and guarantees the tracking of a desired heading direction. The design of a control force that weighs attitude errors improves significantly the transient performance, in terms of position overshoot, compared to existing approaches. Finally, our method avoids by design degenerate conditions that affect other approaches, specifically for what concerns the computation of the reference attitude. Future works will address the possibility of exploiting more aggressive position stabilizers than those based on nested saturations.

REFERENCES

[1] F. Bullo and Murray R. M. Tracking for fully actuated mechanical systems: a geometric framework. *Automatica*, 35(1):17–34, jan 1999.

[2] G. J. J. Ducard and M.-D. Hua. Discussion and pratical aspects on control allocation for a multi-rotor helicopter. *ISPRS - International Archives of the Photogrammetry, Remote Sensing and Spatial Information Sciences*, XXXVIII-1/C22:95–100, 2011.

[3] R. Goebel, R. G. Sanfelice, and A. R. Teel. *Hybrid Dynamical Systems*. University Press Group Ltd, 2012.

[4] M.-D. Hua, T. Hamel, P. Morin, and C. Samson. A control approach for thrust-propelled underactuated vehicles and its application to VTOL drones. *IEEE Transactions on Automatic Control*, 54(8):1837–1853, 2009.

[5] M.-D. Hua, T. Hamel, P. Morin, and C. Samson. Introduction to feedback control of underactuated VTOL vehicles: A review of basic control design ideas and principles. *IEEE Control Systems*, 33(1):61–75, 2013.

[6] D. Invernizzi and M. Lovera. Geometric tracking control of a quadcopter tiltrotor UAV. In *20th IFAC World Congress, Toulouse, France*, 2017.

[7] T. Lee, M. Leok, and H. McClamroch. Geometric tracking control of a quadrotor UAV on SE(3). In *IEEE Conference on Decision and Control, Atlanta, USA*, 2010.

[8] M. Maggiore, M. Sassano, and L. Zaccarian. Reduction Theorems for Hybrid Dynamical Systems. *arXiv:1712.03450*, 2017.

[9] Mahony, R., Kumar, V. and Corke, P. Multirotor Aerial Vehicles: Modeling, Estimation and Control of Quadrotor. *IEEE Robotics & Automation Magazine*, 19(3):20–32, 2012.

[10] R. Naldi, M. Furci, R. G. Sanfelice, and L. Marconi. Robust global trajectory tracking for underactuated VTOL aerial vehicles using inner-outer loop control paradigms. *IEEE Transactions on Automatic Control*, 62(1):97–112, 2017.

[11] A. Roza and M. Maggiore. A class of position controllers for underactuated VTOL vehicles. *IEEE Transactions on Automatic Control*, 59(9):2580–2585, 2014.